AAPS PharmSciTech (2022) 23: 164
https://doi.org/10.1208/s12249-022-02287-9

RESEARCH ARTICLE

Theme: Inhaled Drug Delivery of Biologics for Therapeutic and Vaccination

Dry Powder Inhalers Based on Chitosan-Mannitol Binary Carriers: Effect of the Powder Properties on the Aerosolization Performance

Ziyu Zhao[1] · Guanlin Wang[1] · Zhengwei Huang[2] · Ying Huang[2] · Hangping Chen[2] · Xin Pan[1] · Xuejuan Zhang[2]

Received: 21 February 2022 / Accepted: 18 April 2022 / Published online: 14 June 2022

Abstract

Carriers play an important role in improving the aerosolization performance of dry powder inhalers (DPIs). Despite that intensive attention had been paid to the establishment of the advanced carriers with controllable physicochemical properties in recent years, the design and optimization of carrier-based DPIs remain an empiricism-based process. DPIs are a powder system of complex multiphase, and thus their physicochemical properties cannot fully explain the powder behavior. A comprehensive exposition of powder properties is demanded to build a bridge between the physicochemical properties of carriers and the aerosolization performance of DPIs. In this study, an FT-4 powder rheometer was employed to explore the powder properties, including dynamic flow energy, aeration, and permeability of the chitosan-mannitol binary carriers (CMBCs). CMBCs were self-designed as an advanced carrier with controllable surface roughness to obtain enhanced aerosolization performance. The specific mechanism of CMBCs to enhance the aerosolization performance of DPIs was elaborated based on the theory of pulmonary delivery processes by introducing powder properties. The results exhibited that CMBCs with appropriate surface roughness had lower special energy, lower aeration energy, and higher permeability. It could be predicted that CMBC-based DPIs had greater tendency to fluidize and disperse in airflow, and the lower adhesion force between particles enabled drugs to be detached from the carrier to achieve higher fine particle fractions. The specific mechanism on how physicochemical properties influenced the aerosolization performance during the pulmonary delivery processes could be figured out with the introduction of powder properties.

KEY WORDS dry powder inhalers · powder properties · particle physicochemical properties · pulmonary delivery processes · aerosolization performance · FT-4 powder rheometer

INTRODUCTION

Dry powder inhalers (DPIs) are a promising pulmonary drug delivery system with the advantages of local delivery, fast acting, and satisfactory patient compliance, which have been widely employed in the treatment of pulmonary diseases (1). DPIs can be divided into carrier-based DPIs and carrier-free DPIs. At present, more than 90% of the DPIs on the market contain carriers, assigned as carrier-based DPIs (2). Carriers are beneficial to improve the flowability and physicochemical stability of DPIs. It has been reported that carriers exert a significant influence on the aerosolization performance of DPIs (3), rendering the design and optimization of advanced carriers a research hotspot.

In recent years, a variety of advanced carriers have been constructed by altering the physicochemical properties, including particle size, morphology, density, porosity, and surface roughness (2, 4–10). These studies have explored the aerosolization performance enhancement mechanism dependent of physicochemical properties, and attempted to clarify the key factors in improving aerosolization performance to further optimize the advanced carriers. However, DPIs are a

Ziyu Zhao and Guanlin Wang made equal contributions to this work.

✉ Ying Huang
huangy2007@163.com

✉ Xuejuan Zhang
zhanghongdou0223@126.com

[1] School of Pharmaceutical Sciences, Sun Yat-Sen University, Guangzhou 510006, Guangdong, People's Republic of China

[2] College of Pharmacy, Jinan University, Guangzhou 510632, Guangdong, People's Republic of China

complex multiphase powder system. It is difficult to describe the entire complex only by their physicochemical properties. From this standpoint, the established aerosolization performance enhancement mechanisms were often inconclusive and contradictory, resulting in that the design and optimization of advanced carriers still remain an empiricism-based process. For instance, Kaialy *et al*. (11) reported that the increase of carrier surface roughness reduced the adhesion between drug and carrier, and improved the aerosolization performance. In contrast, Flament *et al*. (12) asserted that there was a negative correlation between carrier surface roughness and aerosolization performance.

Of note, it is the powder properties rather than the physicochemical properties that can directly affect the pulmonary delivery processes driven by airflow (6, 7). The aerosolization performance enhancement mechanism of advanced carriers is expected to be clarified successively by a comprehensive and in-depth exploration of powder properties. Regrettably, the evaluations for physicochemical properties have been well established, but those for powder properties lag far behind. The angle of repose (13), Carr index (14), pore flow velocity (15), etc., are used to describe the powder properties in traditional solid-state pharmaceuticals. It is important to note that DPI powder needs to fluidize, disperse, and eventually settle deep in the lungs during the respiratory drive, and thus those above indicators cannot accurately and objectively evaluate the powder for fluidization and transportation of DPIs due to the absence of airflow. This is also the decisive reason why the advanced carriers were mainly constructed via altering the physicochemical properties.

The FT-4 powder rheometer is an innovative technology for powder property characterization (16), which provides a comprehensive assessment to the powder behavior in the dynamic process, including dynamic flow, aeration, and permeability. Compared with conventional characterization methods, the FT-4 powder rheometer supplies an opportunity to accurately model and predict the multiphase system of DPIs (17). Specifically, basic flow energy, aeration energy, and permeability can be directly quantified by measuring the energy of a helical blade going through powder with axial and rotational forces, which can reflect the powder properties in flowing state (18–20). Therefore, the FT-4 powder rheometer is expected to clarify the mechanism of advanced carriers improving the DPI aerosolization performance by evaluating the powder properties of DPIs.

A suitable model DPI should be selected for FT-4 analysis. Chitosan-mannitol binary carriers (CMBCs), fabricated via one-step spray drying as an advanced carrier to explore the effect of surface roughness on DPI aerosolization performance in our previous study (21), are a promising candidate. CMBCs are a binary system with diverse surface roughness scales, which was formed based on the difference in molecular migration rates of the two components (chitosan and mannitol) during evaporation. It has been confirmed that the *in vitro* and *in vivo* aerosolization performance of CMBC-based DPIs was remarkably improved with the appropriate adjustment of particle surface roughness. Nevertheless, the mechanism of CMBCs improving the aerosolization performance has not been clarified, which brings difficulties to the further and expanding application of this system.

In this study, the FT4 powder rheometer was employed to explore the powder properties of CMBCs, including dynamic flow energy, aeration, and permeability. Furthermore, the relationship between powder properties, particle physicochemical properties, and DPI aerosolization performance was explored to elaborate the specific mechanism improving the aerosolization performance based on the theory of pulmonary delivery processes. This work provides new insights for the design and optimization of advance carriers, which is of great significance for the development of DPIs.

MATERIALS AND METHODS

Materials

Budesonide (BUN, 99.2% purity) was selected as the model drug and purchased from Chu Feng Yuan Technology Co., Ltd. (Wuhan, China). Mannitol (MAN, analytical grade) was obtained from Da Mao Chemical Reagent Factory (Tianjin, China). Chitosan hydrochloride (CTH, deacetylation degree 90.2%, viscosity 28 cps) was purchased from Aokang Biological Technology Co., Ltd. (Weihai, China). Acetonitrile (HPLC grade) was obtained from Thermo Fisher Scientific (Pittsburgh, American). Other chemicals were of analytical grade.

Preparation of CMBCs

CMBCs with different CTH-MAN ratios (Table I) were fabricated via a documented spray-drying method (21). Briefly, MAN with or without CTH was dissolved in 30% (*v*/*v*) ethanol–water solution to obtain a total concentration of 20 mg/

Table I Formulations of CMBCs with Different Mannitol-Chitosan Ratios

Formulation	MAN	$CMBC_1$	$CMBC_2$	$CMBC_3$	$CMBC_4$	$CMBC_5$
MAN (%)	100	90	70	50	30	10
CTH (%)	0	10	30	50	70	90

mL, and then spray-dried using an EYELA SD-1000 spray-dryer (Tokyo Rikakikai Co., Ltd., Tokyo, Japan). The spray-dryer was operated under the following parameters: nozzle tip 0.71 mm, feed rate 7 mL/min, inlet temperature 140 °C, outlet temperature 85 °C, gas flow rate 0.6 m^3/min, and aspirator pressure 150 kPa.

CMBC Surface Roughness Measurement

The surface roughness of CMBCs was measured by atomic force microscopy (AFM, SPM-9500J3, Shimazu Institute, Japan). The AFM contact mode is adopted. The maximum scanning range and scanning frequency were 10 μm × 10 μm and 1.52 Hz, respectively. After obtaining the original surface topography image, the scans were analyzed with the NanoScope Analysis software version 1.40r1.

Powder Property Measurement

It was primary to assess the powder properties and further determine the crucial factors affecting aerosolization performance, in order to elucidate the aerosolization performance enhancement mechanism. In this study, the FT4 powder rheometer was employed to explore the flowability, adhesion force, and dispersion of carrier by dynamic test, aeration test, and permeability test, respectively.

The standard dynamic test, aeration test, and permeability test were determined with the FT-4 powder rheometer (Freeman Technology Ltd., Tewkesbury, UK) according to previously reported methods with proper modifications (7). All the measurements were performed in triplicate.

Dynamic Test

The dynamic properties were determined by measuring the resistance of helical blades as they rotated and moved axially into the powder at a constant velocity. Firstly, about 30 mL sample powder was filled into the vessel for pretreatment and precisely weighed. During the dynamic test processing, there were 11 test cycles in total. The tip speed in the first 7 identical test cycles was 100 mm/s, while the tip speed in the last 4 cycles were 100, 70, 40, and 10 mm/s, respectively. The flowability of powder was quantitatively expressed by total energy (TE), which was calculated by the rotational torque and the axial force of powder on blade. In addition, several important parameters measured with the standard dynamic test are defined in Table II.

Aeration Test

For the aeration test, about 30 mL sample powder was filled into the vessel with a special inflatable base for pretreatment, and then procedures similar to the dynamic test were carried out, under the condition where the powder was filled with air from the bottom. Noticeably, the flow rate of air was 0, 2, 4, 6, 8, and 10 mm/s successively in the whole test process while the helical blades moved at the speed of 100 mm/s, and the flow energy of powder under different air velocities was recorded. According to the flow energy curve of the aeration test, a constant minimum was obtained as the increase of the flow rate which meant that the powder was totally fluidized. The aeration properties were quantitatively assessed by aerated energy (AE) and aeration ratio (AR). AE was defined as the flow energy to move the blade through the powder under the airflow of 10 mm/s, while AR was the ratio of the flow energy at 0 mm/s flow rate to AE.

Permeability Test

Permeability test was employed to evaluate the ability of air penetration through powders. After a similar pretreatment as the test abovementioned, different normal stresses (0, 2, 4, 6, 8, 10, 12, and 15 kPa) were applied to the powder while 2 mm/s air flow was introduced constantly from the vented base. The corresponding pressure drop values for different applied normal stresses were recorded to calculate the corresponding permeability (22). The poor permeability could be reflected by a higher-pressure drop.

Table II Dynamic Testing — Parameter, Units, Definition, and Calculation

Parameter	Unit	Definition	Calculation
Basic flow energy (BFE)	mJ	The energy needed to displace a conditioned powder sample during downwards testing	$BFE = TE_{test-7}$
Special energy (SE)	mJ/g	The energy per gram needed to displace conditioned powder during upwards testing	$SE = {TE_{test-6} + TE_{test-7}}/{2m}$
Stability index (SI)	-	The factor by which the measured flow energy changes during repeated testing	$SI = {TE_{test-7}}/{TE_{test-1}}$
Flow rate index (FRI)	-	The factor by which the flow energy is changed when the tip speed is reduced, reflecting the sensitivity of powder to air flow rate	$FRI = {TE_{test-11}}/{TE_{test-8}}$

Preparation of CMBC-Based DPIs

To obtain DPIs, BUN was first micronized to $d_{50} < 2$ μm and then mixed with CMBCs to enable drug delivery to the deep lung. Specifically, BUN was micronized by air jet milling (Youte Powder Mechanical Equipment Co. Ltd., Yixing, China) with the ring pressure and venturi pressure of 0.40 MPa and 0.45 MPa, respectively. Then, micronized BUN and CMBCs were manually mixed (1:20, w/w) for 5 min to obtain CMBC-based DPIs, which were packed into 3# hard hydroxypropyl methylcellulose capsules (Suzhou Capsugel Co., Ltd., Suzhou, China) after being precisely weighed (10.0 ± 0.5 mg).

In Vitro Aerosolization Performance

The *in vitro* aerosolization performance of DPI formulations was determined with a next-generation impactor (NGI, Copley Scientific Ltd., Nottingham, UK) as previously described (21). Briefly, the test was carried out at the flow rate of 60 L/min, and the cutoff diameters of the NGI stages (stage 1 ~ 7 and MOC) are shown in Table III. A capsule loaded in TurboSpin™ was tested for 4 s, ten capsules were used in each run, and three replicates were carried out for each formulation. BUN deposited on the NGI cups was collected with a certain amount of ethanol and quantitatively determined by high-performance liquid chromatography (HPLC) (21). The fine particle fraction (FPF) was calculated by CITDAS® software (version 3.10, Copley Scientific Ltd., Nottingham, UK), which was an important indicator to evaluate the aerosolization performance of DPIs.

Results Expression and Statistics

All data was reported as mean ± standard deviation (S.D.), if possible. SPSS 20 software (IBM Corporation, Armonk, NY) was conducted for statistical analyses. The skewness and homogeneity of variance were tested before further comparison. One-way analysis of variance (ANOVA) or chi-square tests were performed to compare the obtained data, and $p < 0.05$ was considered as significant difference.

RESULTS

Surface Roughness of Carrier

The CMBCs with different surface roughness scales were designed to obtain excellent aerosolization performance in our previous study. As shown in Fig. 1, the single component of MAN had a smooth surface, while CMBCs had a rough surface. With the increase of chitosan proportion, the surface roughness of CMBCs increased gradually. According to the calculation results of *R*a and *R*q (Fig. 1B), $CMBC_2$ consisted of 70% mannitol and 30% chitosan, which had the roughest surface. It was

Table III The Cutoff Diameters of the NGI Stages at a 60-L/min Flow Rate

	Stage 1	Stage 2	Stage 3	Stage 4	Stage 5	Stage 6	Stage 7	MOC
Cutoff diameters (μm)	> 08.06	4.46 ~ 8.06	2.82 ~ 4.46	1.66 ~ 2.82	0.94 ~ 1.66	0.55 ~ 0.94	0.34 ~ 0.55	< 0.34

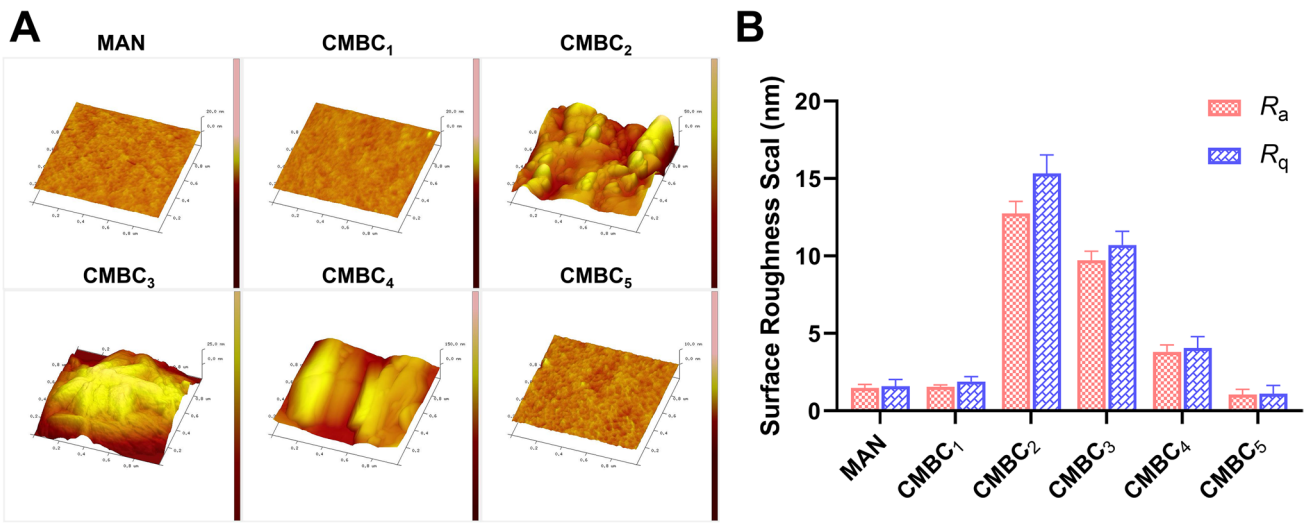

Fig. 1 The surface roughness of MAN and CMBCs. **A** AFM images of CMBCs. **B** Calculated *R*a and *R*q values for CMBCs

noteworthy that when the proportion of chitosan was too high, there was a smoother surface that was close to a single component (chitosan). The difference in molecular migration rates between mannitol and chitosan contributes to the rough surface of CMBCs. However, when the surface roughness of the CMBCs changed, the particle size and other physicochemical properties could change correspondingly due to the limitations of the preparation method. All the above physicochemical properties might have an unpredictable impact on the aerosolization performance, which made it difficult to evaluate the effect of each single physicochemical property on the aerosolization performance of CMBC-based DPIs. It was necessary to comprehensively evaluate the powder properties to clarify the effect of CMBC surface roughness on the aerosolization performance.

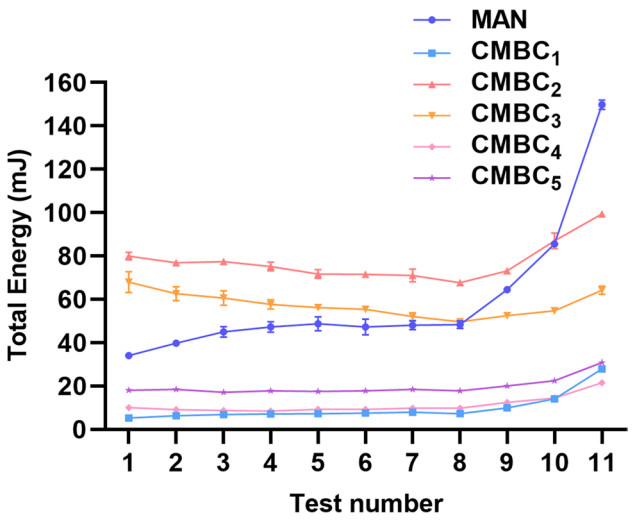

Fig. 2 The dynamic profiles of MAN and CMBCs ($n=3$)

Powder Properties of Carriers

Dynamic Flow Property of Carriers

The dynamic profiles of CMBCs are demonstrated in Fig. 2. TE was roughly constant during the initial 7 cycles but increased significantly in the last 4 cycles as the blade speed dropped. As reported by Freeman Technology (23), TE reflected the resistance to the flow of powder, and hence the resistance of the blades increased gradually as the tip speed decreased; a lower TE value indicated better flowability of powder in general.

Based on TE values in the standard dynamic flow test, BFE, SE, SI, and FRI could be calculated, which were key parameters to evaluate powder flowability. Specifically, the TE values for the initial 7 cycles were defined as BFE. As shown in Fig. 3A, BFE values of $CMBC_1$ and $CMBC_{4\sim5}$ were significantly lower than MAN ($p<0.05$), but $CMBC_{2\sim3}$ have the highest BFE values. It was worth noting that BFE was the energy required to displace a conditioned powder as the blades moved downward, which was associated with dynamic flowability, bulk compressibility, and powder consolidation level (24). For the cohesive powders with smoother surface and smaller particle size (21) such as MAN, $CMBC_1$, and $CMBC_5$, the low BFE value suggested good flow properties; in contrast, powders exhibiting high BFE values were often associated with poor flowability (25). However, a higher BFE value could be measured for non-cohesive powders or powders with larger d_{ae}, despite the fact that the flow properties might be acceptable (26). A possible explanation was that the flowing zone around the blade was extensive due to the low compressibility of the powder and the high transmissibility of forces between particles, and for this reason a higher flow energy was required to start the powder flow. Therefore, the sharp rise of BFE for $CMBC_{2\sim3}$ might be the results of surface roughness and particle size increase.

With regard to SE values (Fig. 3B), $CMBC_{1\sim5}$ were obviously lower than MAN, indicating that the modification of

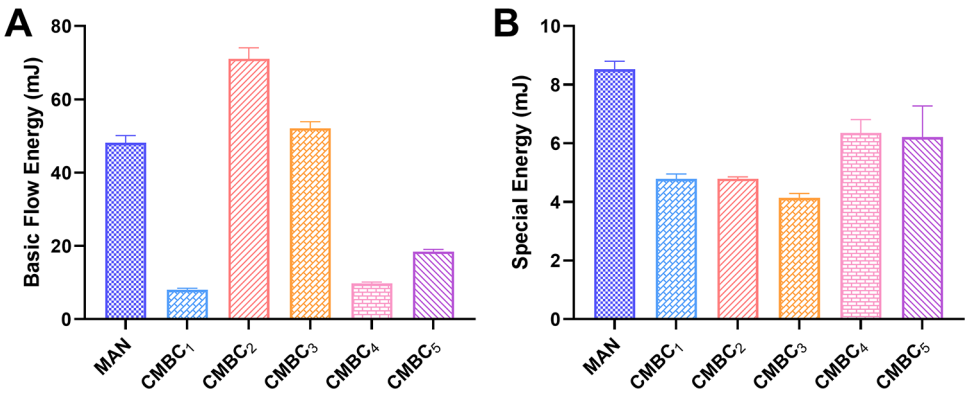

Fig. 3 The dynamic test results of MAN and CMBCs. **A** Basic flow energy (BFE) values of MAN and CMBCs. **B** Special energy (SE) values of MAN and CMBCs ($n=3$)

CMBCs effectively reduced the inter-particulate cohesion and consequently improved the flow properties of powder. SE was obtained during the upwards testing where the powder was not constrained by space. It was generally observed that powder exhibiting low SE values had good flow property since SE was mainly related to intrinsic particle properties, such as cohesion, particle size, and surface roughness (25). Specifically, the significant lower SE values of $CMBC_{1\sim5}$ might be explained by the reduction of the interparticle contact area owing to the increase of surface roughness and particle size (Fig. 1) (21). Furthermore, the appearance of surface roughness might make a very positive contribution to the fact that SE values of $CMBC_{1\sim3}$ were slightly lower than $CMBC_{4\sim5}$ ($p<0.05$), and therefore the powder had lower tendency to aggregate and better dispersion performance.

Additionally, SI was calculated to estimate the stability of physical properties during repeated testing. As shown in Fig. 4A, SI values of $CMBC_{2\sim5}$ were significantly lower than MAN ($p<0.05$), and $CMBC_{2\sim3}$ had the lowest SI values. SI was the ratio of $TE_{test\text{-}7}$ to $TE_{test\text{-}1}$, and a value closer to 1 reflected better powder stability. The SI value higher than 1 stood for that powder aggregation might occur during the repeated testing, and conversely that less than 1 indicated the presence of disaggregation. The remarkable lower SI values of $CMBC_{2\sim3}$ might be attributed to the increase of surface roughness, which reduced the contact area and interparticulate forces between particles. Hence, $CMBC_1$ might be easier to aggregate during the preparation of carrier-based DPIs, and the lowest SI values of $CMBC_{2\sim3}$ indicated that the powder was able to disaggregate from complex powder generated by pretreatment, which had great advantages in the process of mixture, transportation and fluidization of DPIs.

As described in Fig. 4B, $CMBC_{2\sim5}$ had lower FRI values than MAN, and FRI values of $CMBC_{2\sim3}$ were the lowest, similar to the results of SI. It was reported that FRI was used to assess the effect of blade speed on powder cohesion, and generally a high FRI value was resulted from the excessive sensitivity to stress (27). It had been reported that the FRI value below 3 was desirable (28). The FRI values of MAN and $CMBC_1$ were higher than the critical value 3, while those of $CMBC_{2\sim5}$ were satisfactory. The higher FRI value indicated that TE increased rapidly with the decrease of blade speed, which was consistent with the characteristic of cohesive powder. A possible explanation for the particle with smooth surface requiring greater flow energy at lower flow rates was that the inter-particulate interstice was finite, leaving a stiffer material with more resistance to flow (25). Conversely, the non-cohesive powder with suitable surface roughness was much less sensitive to blade speed, because the void space and the contact between particles remained more or less unaffected by the blade speed and the bulk density remained unchanged. Therefore, $CMBC_{2\sim5}$ were less sensitive to the blade speed, indicating that powder has low possibility to aggregate and consolidate spontaneously.

Aeration Test

It was insufficient to evaluate the powder properties without airflow by the traditional evaluations, for the reason that the delivery of DPIs was a dynamic process always with the presence of airflow. The aeration test was an important extension of the standard dynamic test, which introduced air into the base of the powder column and quantified the effect of airflow on flow properties by measuring the reduction in flow energy (28). Figure 5 shows the variation of the flow energy with air velocity, and significant differences in aeration behaviors were evidenced between all 6 powders. The results showed that with the increase of airflow velocity, the interior of $CMBC_{1\sim4}$ presented a fluidized state, and flow energy gradually decreased until it reached a steady state. Among them, the flow energy of $CMBC_2$ and $CMBC_3$ decreased rapidly to a steady state under the airflow of 2 mm/s, indicating that they had satisfactory flow and dispersion properties at a relatively low airflow speed, and were especially suitable for the delivery of DPIs. In addition, $CMBC_1$ and $CMBC_4$ could still reach a relatively

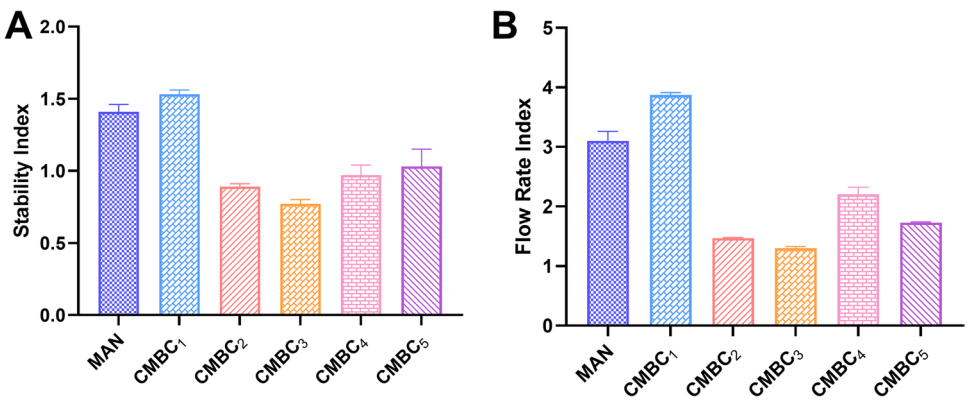

Fig. 4 The dynamic test results of MAN and CMBCs. **A** Stability index (SI) values of MAN and CMBCs. **B** Flow rate index (FRI) values of MAN and CMBCs ($n=3$)

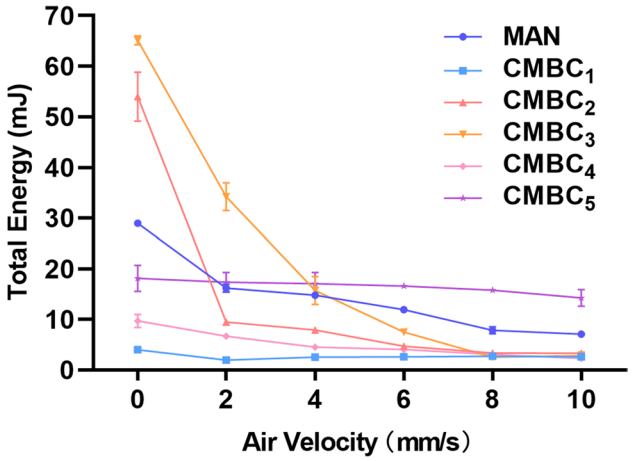

Fig. 5 Aeration test of MAN and CMBCs ($n=3$)

steady state under the airflow of 8 mm/s though their initial flow energy was slightly lower, indicating that their dispersion was better than that of MAN. It was worth noting that the flow energy of MAN could decrease continuously with the increase of airflow velocity, although it failed to reach a steady state even under the flow of 10 mm/s, reflecting that MAN had a relatively satisfactory dispersion performance. However, the flow energy of $CMBC_5$ had little change even under the airflow of 10 mm/s, which meant that the pneumatic transmission and dispersion properties hampered the industrialization process. It was speculated that the powder with higher content of chitosan appeared to consolidate, and the air could not penetrate the whole sample but overflowed from some fixed concave or pores, and thus the flow energy was unchanged with the increase of airflow rates.

From these results, aerated energy (AE) and aerated ratio (AR) were obtained. As shown in Fig. 6A, AE values of $CMBC_{1\sim4}$ were significantly lower than those of MAN ($p<0.05$). AE was the flow energy to move the blade through the powder under the airflow of 10 mm/s. Generally, AE was used as an indicator to evaluate the cohesion strength of powder with the presence of airflow, and a low AE value represented excellent fluidization and dispersion performance. The weaker cohesion of CMBCs might be caused by the rough surface of CMBCs. It had been studied that the contact area of particles with a rough surface was smaller than those with a relatively smooth surface (29), and thus the powder had a weaker cohesion.

Further, the ratio of BFE to AE was defined as AR, which reflected the sensitivity of powder to air flow, and the powder with a larger AR value tended to readily reach a fluidized state. Coincidentally, $CMBC_2$ and $CMBC_3$ had both lower AE and larger AR than MAN, reflecting that $CMBC_2$ and $CMBC_3$ had satisfactory flowability, fluidization, and dispersion properties. In contrast, AR values of $CMBC_1$ and $CMBC_{4\sim5}$ were lower than those of MAN ($p<0.05$), indicating that their flowability in airflow condition was not satisfactory, though they performed well in the standard dynamic test. The differences of AE and AR between the powders mentioned above could be obligated to the variation of surface roughness. The dimples and holes on the surface of particles gave rise to the disorder and abruption of airflow to a greater extent, leading to a large pressure difference and turbulent flow between particles, and thus lift and suspension of the particles occurred at relatively low air velocities (25). According to a previous study (21), $CMBC_2$ and $CMBC_3$ had rougher surface than other powders, confirmed by AFM. For this reason, $CMBC_2$ and $CMBC_3$ had a high sensitivity to even lower airflow, showing a rapid reduction of flow energy.

Permeability

The permeability generally represented the difficulty of powder transmitting air under certain pressure conditions, and reflected the fluidization and dispersion performance of carrier-based DPIs. Figure 7 shows the permeability of the powder at 2-mm/s airflow for various applied normal stresses. MAN and $CMBC_1$ had the lowest permeability, which might be attributed to the relatively smoother surface, and consequently the powder was more compacted and air was more difficult to pass through it. It was noteworthy that

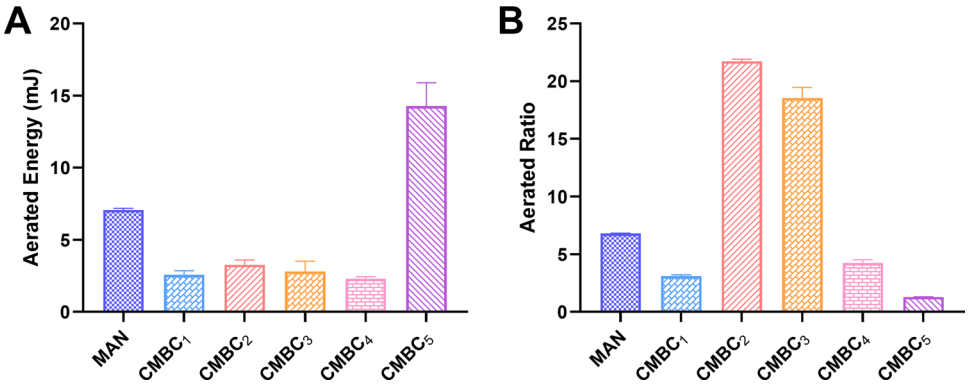

Fig. 6 The aeration test results of MAN and CMBCs. **A** Aerated energy (AE) values of MAN and CMBCs. **B** Aerated ratio (AR) values of MAN and CMBCs ($n=3$)

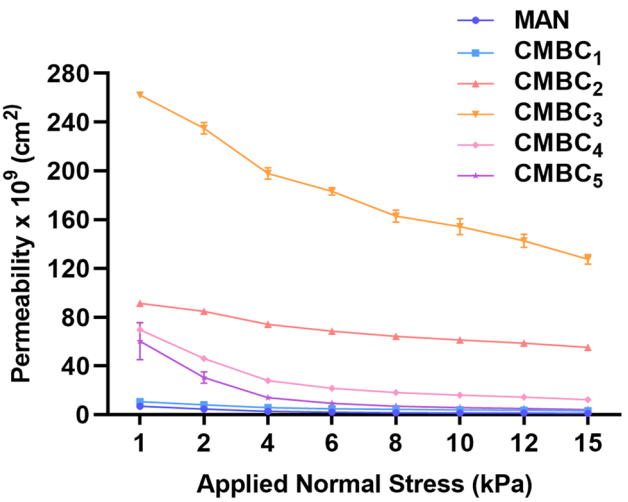

Fig. 7 The permeability of MAN and CMBCs ($n=3$)

a distinctly higher permeability in $CMBC_2$ and $CMBC_3$ was observed when compared to others, consequently exhibiting better fluidization and dispersion performance. This was owing to the higher roughness of the particle surface, and there were certain voids inside the powder so that the airflow could pass through the powder with less resistance. Besides, there was a sharp reduction of permeability in $CMBC_3$ with a normal stress increasing from 1 to 15 kPa, suggesting a deterioration of permeability. Additionally, $CMBC_{4\sim5}$ had a relatively poor permeability because of the smooth surface.

The Effect of Powder Properties on *In Vitro* Aerosolization Performance

The aerosolization performance of the CMBC-based DPIs was evaluated by NGI and is shown in Fig. 8. The mass ratio of the active pharmaceutical ingredient (API) within a certain range of impactor cutoff size to all collected API was defined as FPF, which was an important parameter to quantify the aerosolization performance. The results showed that FPF values of CMBC-based DPIs were significantly higher than those of MAN-based DPIs (FPF: 21.67%), elucidating the superior *in vitro* aerosolization performance of CMBC-based DPIs. Besides, DPIs prepared by $CMBC_2$ and $CMBC_3$ had the highest FPF values, viz., 43.56% and 41.42%, respectively. Based on the above studies, the correlation between powder properties and aerosolization performance was further explored. Herein, we had established the correlation between AR and FPF in binary carrier CMBCs. As shown in Fig. 8B, there was a positive correlation between AR and FPF, indicating that a better permeability was desirable in pulmonary delivery processes. There was no doubt that the enhanced aerosolization performance of CMBC-based DPIs could be ascribed to the change of surface roughness and particle size, which results in the increase of inter-granular voids. The presence of voids made it easier for airflow to pass through the powder and reduced the adhesion force between particles. Correspondingly, the CMBC-based DPIs had greater tendency to fluidize and disperse in airflow, and the API could be detached from the carrier in bronchioles to achieve excellent aerosolization performance.

DISCUSSION

Currently, it is difficult to establish a mathematical model to accurately predict the effect of surface roughness and particle size on aerosolization performance due to the presence of multivariable particles. The optimization of CMBCs still remains an empirical and uncontrollable process, which constructs enormous barriers to the further and expanding application of CMBCs. Powder properties showed more relevance with the pulmonary delivery processes than physicochemical properties, according to the enriched theory revealed in our previous study via the self-built modular platform (30).

Generally, the pulmonary delivery processes can be roughly described by four consecutive stages: fluidization-dispersion, transportation, detachment, and deposition. The sequential and efficient achievement of the four stages is the guarantee of superior aerosolization performance.

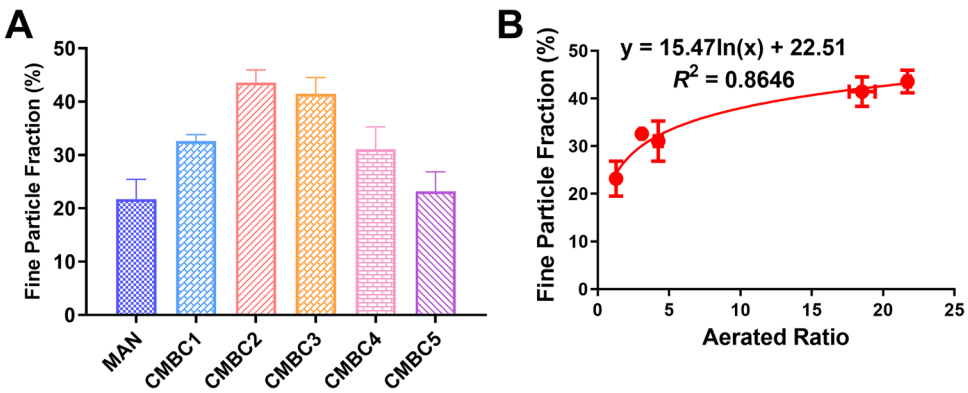

Fig. 8 *In vitro* aerosolization performance test of CMBC-based DPIs by NGI (60 L/min, 4 s, $n=3$). **A** The FPF values of CMBC-based DPIs. **B** The correlation between AR and FPF

Firstly, DPIs should be fluidized and dispersed through airflow generated by breathing, which can be assessed by aeration test and permeability test. The powders that can be fluidized rapidly at lower airflow are probable to achieve satisfactory dispersion. According to the results of the aeration test, AE values of $CMBC_{1\sim4}$ were lower than those of MAN ($p < 0.05$), which meant that the $CMBC_{1\sim4}$-based DPIs had better fluidization and dispersion behavior even under lower airflow conditions. On the contrary, $CMBC_5$ and MAN required a higher airflow to achieve acceptable fluidization and dispersion, resulting in a premature deposition of the API-carrier complex in the DPI device or upper respiratory tract. Interestingly, this inference was supported by the results of permeability. MAN which performed poorly in the aeration test had the lowest permeability, resulting in undesired fluidization and dispersion of the inner powder. In addition, though the aeration of $CMBC_1$ and $CMBC_{4\sim5}$ was relatively acceptable, their permeability was dissatisfactory, corresponding to the lower FPF values. It was indicated that satisfactory fluidization and dispersion can be achieved only with lower aeration and higher permeability, like $CMBC_2$ and $CMBC_3$. In addition, the stability and flowability of the powders of CMBCs and CMBC-based DPIs were also important factors to be considered, which had an important influence on fluidization and dispersion processes. According to the results of the dynamic test, the flow energy of MAN and $CMBC_1$ increased obviously ($p < 0.05$), in accordance with higher SI values (1.41 and 1.53, respectively). In other words, MAN and $CMBC_1$ had poor stability in the mixing and pre-compression process, and the particles tended to aggregate. At the same time, the SE values of $CMBC_{2\sim3}$ were lower than those of $CMBC_{4\sim5}$, while the BFE values were higher, indicating that the powder of $CMBC_{2\sim3}$ had preeminent flowability and dispersion performance. For particles with a relatively smoother surface, aggregation may occur when inhaled by patients owing to excessive contact area and finite inter-particulate intervals. However, particles with a rough surface have weak cohesion and are more likely to reach a fluidized state.

After fluidization and dispersion, the drug-carrier complex will be transported to the oropharynx region, trachea, and bronchi sequentially (31). With the narrowing of bronchioles, the shear force of airflow becomes high enough for API to detach from the surface of carrier particles. The transportation of the drug-carrier complex and the detachment of drug from the carrier are mainly associated with the aerodynamic properties of powder and relative strength of cohesion force (32, 33). On the one hand, if the cohesion force between API and carrier is weak, the API will detach from the complex early, and deposit in the upper respiratory tract rather than the deep lung. On the other hand, excessive cohesion will cause the API to be difficult to detach from the complex, and finally be trapped in the bronchi and removed by cilia action or swallowed due to the larger particle size. In this work, the SE and AE were adopted to estimate the relative strength of cohesion force. Lower SE and AE values made $CMBC_{2\sim3}$ have a lower cohesion, and API could timely detach from the surface of carriers. It was worth noting that $CMBC_3$ had the lowest SE and AE values, but the FPF value of $CMBC_3$-based DPIs was slightly lower than that of $CMBC_2$-based DPIs. The contradictory results might be triggered by the excessively weak cohesion force of $CMBC_3$. Based on the above results, the cohesion of $CMBC_2$ was stronger than that of $CMBC_3$, which was more suitable for the transportation and detachment of API-carrier complexes. In conclusion, a too strong or too weak cohesion will lead to premature deposition of the API in the upper respiratory tract, and an appropriate cohesion is needed to ensure a tight binding of the transportation process and timely detachment in bronchioles.

As indicated by the current results, lower aeration, higher permeability, superior stability, and flowability all contribute to the satisfactory fluidization and dispersion. Besides, appropriate cohesion avoids premature deposition of the API in the transportation and detachment processes. All the above factors contribute to the pulmonary delivery processes, and ultimately achieve the enhancement aerosolization performance of CMBC-based DPIs. In conclusion, powder properties are potential indicators for the design and optimization of advanced carriers, and their effects on pulmonary delivery processes need to be taken into consideration seriously.

CONCLUSION

The design and optimization of advanced carriers with various physicochemical properties are research hotspots for carrier-based DPIs. However, the design and optimization of advanced carriers which are mainly focused on physicochemical properties, remaining an empiricism-based process. In the present study, CMBCs, an advanced carrier was employed to explore the effect of particle physicochemical properties on aerosolization performance by measuring powder properties, including dynamic flow energy, aeration energy, and permeability via a FT4 powder rheometer. The enhancement mechanism of powder properties on improving the aerosolization performance was further explored based on the theory of pulmonary delivery processes. It was considered that the superposed impact of satisfactory flowability, superior stability, lower aeration energy, higher permeability, and appropriate adhesion force contributed to the aerosolization performance enhancement of CMBC-based DPIs. The results showed that powder properties provided a novel insight to explain the influence of physicochemical properties on aerosolization performance. This study

provided a novel insight for the design and optimization of advanced carriers, and had great significance to the development of carrier-based DPIs loading different cargoes like antitumor drugs, macromolecules, and nanoparticles.

Acknowledgements The authors would like to thank the help in the FT4 instrument and data analysis from Freeman Technology Ltd.

Author Contribution Ziyu Zhao conducted the experiments and revised the manuscript. Guanlin Wang analyzed the data and wrote the paper. Zhengwei Huang analyzed the data and helped to design the study. Ying Huang and Hangping Chen helped to design the study and revised the manuscript. Xin Pan and Xuejuan Zhang designed and supervised the study and proofread the manuscript.

Funding The authors were funded by the National Science Foundation of China under Grant No. 82104072 and No. 82104070; the Fundamental Research Funds for the Central Universities of China under Grant No. 21621014; and the Science and Technology Foundation Guangdong under Grant No. 2021A0505080011.

Declarations

Conflict of Interest The authors declare no competing interests.

References

1. Cazzola M, Cavalli F, Usmani OS, Rogliani P. Advances in pulmonary drug delivery devices for the treatment of chronic obstructive pulmonary disease. Expert Opin Drug Deliv. 2020;17(5):635–46.
2. Yeung S, Traini D, Lewis D, Young PM. Dosing challenges in respiratory therapies. Int J Pharm. 2018;548(1):659–71.
3. Zhao Z, Huang Z, Zhang X, Huang Y, Cui Y, Ma C, Wang G, Freeman T, Lu X-Y, Pan X. Low density, good flowability cyclodextrin-raffinose binary carrier for dry powder inhaler: anti-hygroscopicity and aerosolization performance enhancement. Expert Opin Drug Deliv. 2018;15(5):443–57.
4. Kou X, Heng PW, Chan LW, Wereley ST, Carvajal MT. Effect of roughness on the dispersion of dry powders for inhalation: a dynamic visualization perspective. AAPS PharmSciTech. 2019;20(7):271.
5. Benke E, Farkas Á, Balásházy I, Szabó-Révész P, Ambrus R. Stability test of novel combined formulated dry powder inhalation system containing antibiotic: physical characterization and in vitro–in silico lung deposition results. Drug Dev Ind Pharm. 2019;45(8):1369–78.
6. Peng T, Lin S, Niu B, Wang X, Huang Y, Zhang X, Li G, Pan X, Wu C. Influence of physical properties of carrier on the performance of dry powder inhalers. Acta Pharmaceutica Sinica B. 2016;6(4):308–18.
7. Zhang X, Zhao Z, Cui Y, Liu F, Huang Z, Huang Y, Zhang R, Freeman T, Lu X, Pan X. Effect of powder properties on the aerosolization performance of nanoporous mannitol particles as dry powder inhalation carriers. Powder Technol. 2019;358:46–54.
8. Shetty N, Park H, Zemlyanov D, Mangal S, Bhujbal S, Zhou QT. Influence of excipients on physical and aerosolization stability of spray dried high-dose powder formulations for inhalation. Int J Pharm. 2018;544(1):222–34.
9. Newman S P, Chan H-K. In vitro-in vivo correlations (IVIVCs) of deposition for drugs given by oral inhalation. Advanced Drug Delivery Reviews, 2020.
10. Shiehzadeh F, Tafaghodi M, Dehghani ML, Mashhoori F, Fazly-Bazzaz BS, Imenshahidi M. Preparation and characterization of a dry powder inhaler composed of PLGA large porous particles encapsulating gentamicin sulfate. Advanced Pharmaceutical Bulletin. 2019;9(2):255–61.
11. Kaialy W, Ticehurst M, Nokhodchi A. Dry powder inhalers: mechanistic evaluation of lactose formulations containing salbutamol sulphate. Int J Pharm. 2012;423(2):184–94.
12. Flament M-P, Leterme P, Gayot A. The influence of carrier roughness on adhesion, content uniformity and the in vitro deposition of terbutaline sulphate from dry powder inhalers. Int J Pharm. 2004;275(1–2):201–9.
13. Momin MA, Tucker IG, Doyle CS, Denman JA, Das SC. Manipulation of spray-drying conditions to develop dry powder particles with surfaces enriched in hydrophobic material to achieve high aerosolization of a hygroscopic drug. Int J Pharm. 2018;543(1–2):318–27.
14. Donovan MJ, Smyth HD. Influence of size and surface roughness of large lactose carrier particles in dry powder inhaler formulations. Int J Pharm. 2010;402(1–2):1–9.
15. Ezzati Nazhad Dolatabadi J, Hamishehkar H, Valizadeh H. Development of dry powder inhaler formulation loaded with alendronate solid lipid nanoparticles: solid-state characterization and aerosol dispersion performance. Drug Development and Industrial Pharmacy, 2015, 41(9): 1431–1437.
16. Huang L, Chen L, Lu X. A comparison of dynamic flowability evaluations of lactose powder by two analyzers. Chinese Journal of Pharmaceuticals. 2016;7:24.
17. Cordts E, Steckel H. Capabilities and limitations of using powder rheology and permeability to predict dry powder inhaler performance. Eur J Pharm Biopharm. 2012;82(2):417–23.
18. Zhou QT, Armstrong B, Larson I, Stewart PJ, Morton DA. Understanding the influence of powder flowability, fluidization and deagglomeration characteristics on the aerosolization of pharmaceutical model powders. Eur J Pharm Sci. 2010;40(5):412–21.
19. Pitchayajittipong C, Price R, Shur J, Kaerger JS, Edge S. Characterisation and functionality of inhalation anhydrous lactose. Int J Pharm. 2010;390(2):134–41.
20. Hsu W-Y, Huang A-N, Kuo H-P. Approach the powder contact force, voidage, tensile stress, wall frictional stress and state diagram of powder bed by simple pressure drop monitoring. Adv Powder Technol. 2020;31(1):433–8.
21. Huang Y, Huang Z, Zhang X, Zhao Z, Zhang X, Wang K, Ma C, Zhu C, Pan X, Wu C. Chitosan-based binary dry powder inhaler carrier with nanometer roughness for improving in vitro and in vivo aerosolization performance. Drug Deliv Transl Res. 2018;8(5):1274–88.
22. Mera JPF, Chiamulera ME, Mantelli MB. Permeability model of sintered porous media: analysis and experiments. Heat Mass Transf. 2017;53(11):3277–85.
23. Nan W, Ghadiri M, Wang Y. Analysis of powder rheometry of FT4: effect of particle shape. Chem Eng Sci. 2017;173:374–83.
24. Ambadipudi VG, Kulyadi GP, Tippavajhala VK. Advances in powder flow characterization by Freeman Technology using FT4 Powder Rheometer. Research Journal of Pharmacy and Technology. 2019;12(11):5536–42.
25. Gnagne E, Petit J, Gaiani C, Scher J, Amani G. Characterisation of flow properties of foutou and foufou flours, staple foods in West Africa, using the FT4 powder rheometer. Journal of Food Measurement and Characterization. 2017;11(3):1128–36.
26. Leturia M, Benali M, Lagarde S, Ronga I, Saleh K. Characterization of flow properties of cohesive powders: a comparative study of traditional and new testing methods. Powder Technol. 2014;253:406–23.
27. Wilkinson S, Turnbull S, Yan Z, Stitt EH, Marigo M. A parametric evaluation of powder flowability using a Freeman rheometer

through statistical and sensitivity analysis: a discrete element method (DEM) study. Comput Chem Eng. 2017;97:161–74.
28. Divya S, Ganesh G. Characterization of powder flowability using FT4–Powder Rheometer. J Pharm Sci Res. 2019;11(1):25–9.
29. Tan B M J, Liew C V, Chan L W, Heng P W S. Particle surface roughness–its characterisation and impact on dry powder inhaler performance. iPulmonary Drug Delivery: Advances, 2015: 199–222.
30. Zhang X, Cui Y, Liang R, Wang G, Yue X, Zhao Z, Huang Z, Huang Y, Geng J, Pan X, Wu C. Novel approach for real-time monitoring of carrier-based DPIs delivery process via pulmonary route based on modular modified Sympatec HELOS. Acta Pharmaceutica Sinica B. 2020;10(7):1331–46.
31. Islam N, Dmour I, Taha MO. Degradability of chitosan micro/nanoparticles for pulmonary drug delivery. Heliyon. 2019;5(5): e01684.
32. Berard V, Lesniewska E, Andres C, Pertuy D, Laroche C, Pourcelot Y. Dry powder inhaler: influence of humidity on topology and adhesion studied by AFM. Int J Pharm. 2002;232(1–2):213–24.
33. Berard V, Lesniewska E, Andres C, Pertuy D, Laroche C, Pourcelot Y. Affinity scale between a carrier and a drug in DPI studied by atomic force microscopy. Int J Pharm. 2002;247(1–2):127–37.